trapped electrons can now be nearer the conduction band and may be excited to it by light of lower energy. As the exposure to ultraviolet light in increased, more electrons will be trapped in the higher impurity levels, and the photoconductivity in the red will increase. This increase will finally saturate when equilibrium is achieved between the number of electrons excited from the impurity levels into the conduction band and the number of electrons being retrapped.

It is the hope of the authors that the results of this investigation will be of material assistance in interpreting the spectral darkening of lead chromate which is now being studied by us in collaboration with A. H. Smith. The results of the latter investigation will be available shortly. A theoretical interpretation of the results of both these experiments will be presented by Dr. Frederick Seitz who initiated this program of research and whose active interest throughout the investigation was largely responsible for its completion.

In conclusion, the authors desire to express their indebtedness to the Krebs Pigments Department of the E. I. duPont de Nemours and Company for financial assistance in the form of a fellowship for one of us (J. E. G.) and for a plentiful supply of carefully prepared lead chromate, and to M. L. E. Chwalow who took an active part in the initial phases of the investigation.

PHYSICAL REVIEW VOLUME 64, NUMBERS 1 AND 2 JULY 1 AND 15, 1943

Intensity Anomalies and Perturbations in the CN Bands

A. T. WAGER*
Ryerson Physical Laboratory, University of Chicago, Chicago, Illinois
(Received April 1, 1943)

The rotational structures of the 0,0 violet and the 9,4 red CN bands, developed by $CHCl_3$ in active nitrogen, are measured on plates from the first and second orders of a 30-ft. grating. The rotational constants of the $b^2\Sigma, v=0$ and the $a^2\Sigma, v=4$ states are in good agreement with the previously published values; those for the $v=9\,^2\Pi$ state are $B'_9=1.5312\pm0.0008$ cm^{-1}, $D'_9=7.408\pm0.002\times10^{-6}$ cm^{-1}. The Λ-doubling in this state, except for four perturbations, can be represented by use of the constants $p_0=+0.01597$ and $q_0=-0.00080$. The value $\gamma'=+0.021$ is determined for the spin doubling in the $b^2\Sigma, v=0$ state. Four perturbations are found at $K=4$, 7, 11, and 15 for $b^2\Sigma$; extra P and R lines separated from the main lines by $\Delta\nu=-0.352$ cm^{-1}, $+0.938$ cm^{-1}, $+1.177$ cm^{-1}, and $+1.212$ cm^{-1}, respectively, appear in both the 0,0 and 0,1 bands of the violet system. In the red system, shifts of the right amount and direction in the lines $Q_1[3\frac{1}{2}]$, $R_1[7\frac{1}{2}]$, $P_1[7\frac{1}{2}]$, $R_2[10\frac{1}{2}]$, $P_2[10\frac{1}{2}]$, and $Q_2[15\frac{1}{2}]$ confirm the assumption that rotational levels of $^2\Pi, v=9$, perturb those of $b^2\Sigma, v=0$, and that the perturbations occur for the K and J values indicated. (Brackets denote upper state J.) The values of the perturbation matrix elements are obtained for the various levels. Some anomalies of the R branch band lines in the range 23–29 of K' values in the 0,0 violet band are mentioned.

The mechanism responsible for the enhancements of the main and extra lines of the 0,0 violet band is discussed. Collisions involving interstate transfer ($^2\Pi\rightarrow a^2\Sigma$) evidently occur, or are enhanced, at each perturbed level; and rapid redistribution of molecules among rotational levels by collisions must also occur. Where spin doublets are resolvable in the violet bands, rotational redistribution occurs without change of spin direction.

INTRODUCTION

Historical

IN 1928, G. Herzberg[1] reported that certain lines are enhanced in the emission of bands of the violet cyanogen system coming from the level $b^2\Sigma$, $v=0$, when excited by active nitrogen. The photographs were taken with a low dispersion instrument. Herzberg proposed fluorescence or collisions of the second kind as a tentative explanation. H. T. Byck,[2] in 1929, confirmed the experimental results; however, he found no evidence for a mechanism related to fluorescence, and therefore restricted the explanation to collisions of the second kind.

M. Fred, in 1932, photographed the above bands in the first order of a 21-ft. grating in this

* Now at Birmingham-Southern College, Birmingham, Alabama.

[1] G. Herzberg, Zeits. f. Physik **49**, 512 (1928).

[2] H. T. Byck, Phys. Rev. **34**, 453 (1929).

laboratory and obtained not only the enhancements mentioned, but also three extra lines in each branch. H. Beutler and M. Fred[3] explained this result by a detailed scheme of energy transfer. They compared the rotational terms of the $b^2\Sigma$, $v=0$ state with those of the $^2\Pi$, $v=9$ state as obtained by extrapolation. The calculations showed that four perturbations might be expected to occur, between $J=3\frac{1}{2}$ and $7\frac{1}{2}$ of $^2\Pi_{3/2}$, $v=9$ and $J=10\frac{1}{2}$ and $15\frac{1}{2}$ of $^2\Pi_{1/2}$, $v=9$ on the one hand, and $K=4$, 7, 11, and 15 in $b^2\Sigma$, $v=0$, on the other hand.

This hypothesis was subjected to an experimental test, a preliminary report of which was presented recently.[4] The description of the procedure and the derivation of the results form the content of this paper.

Excitation by Active Nitrogen

One of the ways to obtain the CN bands is to mix the vapor from carbon compounds with active nitrogen; a low-temperature flame yielding narrow rotational lines of low quantum numbers results from such a mixing. Many investigators[5–9] have worked with active nitrogen, either studying its properties or using it for exciting spectra from admixed gases. The excitation of the CN bands belongs to the second case; the CN is formed as a reaction product of the admixed gas with the active nitrogen. The molecules of this admixed gas must contain carbon atoms.

Active nitrogen itself is a mixture of inert and excited atoms and molecules of nitrogen, and its exact nature is not completely known.[10, 11] Active nitrogen is formed in a discharge through nitrogen, especially by a spark discharge.

The detailed mechanism of the formation of active nitrogen is not completely known. It can be assumed that nitrogen atoms leave the discharge tube when the flow method is used, and that their recombination energy is the source for the excitation of any spectrum. This is in agreement with the long life of active nitrogen. Concerning the formation of the nitrogen atoms in the discharge, our knowledge of excitation processes by electron impact indicates that the direct dissociation of molecules is a rather rare process; therefore, it may be assumed that most of the nitrogen atoms are formed by collisions of two excited nitrogen molecules upon each other. The number of nitrogen molecules excited is proportional to the current density, and, if the cross section of the discharge tube is kept constant, to the current itself. If thus two excited molecules have to interact for the formation of atomic nitrogen, the concentration of atomic nitrogen will be proportional to the square of the current density. The assumption of such a mechanism explains the high efficiency of spark discharges compared to arc discharges in the formation of active nitrogen, as described in the following paragraphs.

The total power that can be impressed on a discharge tube depends on the construction of the tube, and especially on the size and cooling of the electrodes. The limit for constant load is usually given by the seals of the electrodes, occasionally by the softening of the Pyrex walls of the discharge tube. If the discharge is interrupted, then the momentary power input can be increased very much. If, for instance, the current is maintained over only about one-tenth of each cycle of the alternating current (five discharges during each 1/120 sec.), then the current density during this time can be increased approximately by the factor square root of ten; however, the yield of active nitrogen will be increased by a factor of ten with respect to the "steady" alternating current according to the assumption made above.

A further assumption made in this rough calculation is that the lifetime of the excited nitrogen molecules is not much longer than the time of such an interrupted discharge. The time of the spark discharge is of the order of 10^{-3} to 10^{-4} sec., and the lifetime of most kinds of excited molecules is less than 10^{-7} sec., hence such a

[3] H. Beutler and M. Fred, Phys. Rev. **61**, 107 (1942).
[4] A. T. Wager, Phys. Rev. **61**, 107 (1942).
[5] D. E. Debeau, Phys. Rev. **61**, 668 (1942), contains references to energy transfer phenomena in active nitrogen.
[6] Lord Rayleigh, Proc. Roy. Soc. **A176**, 1, 16 (1940). Both articles contain references to previous work.
[7] Reference 1.
[8] P. A. Constantinides, Phys. Rev. **30**, 95 (1927), contains references to E. P. Lewis, R. J. Strutt (Lord Rayleigh), F. Compte, Tiede, Pirani, Oosterhuies and Holst, H. W. Webb, H. A. Messenger, M. N. Saha, R. T. Birge, P. D. Foote, Ruark and Chenault, H. Sponer.
[9] J. Kaplan, Phys. Rev. **54**, 176 (1938); **61**, 202 (1942); Zeits. f. Physik **109**, 744, 750 (1938).
[10] H. Sponer, Zeits. f. Physik **34**, 622 (1925); Nature **117**, 81 (1926); and M. H. Hebb, Phys. Rev. **59**, 925 (1941).
[11] G. Cario and J. Kaplan, Zeits. f. Physik **58**, 769 (1929); also contains references to other work.

rough estimate is allowed. It is also assumed in this explanation that the mechanisms of excitation of the nitrogen molecule and of the formation of nitrogen atoms are the same during a spark discharge as during the period of an arc discharge, and that the difference in efficiency is caused only by the much different current densities.

EXPERIMENTAL PROCEDURE

The experimental problem was to develop a light source yielding CN bands of sufficient intensity to utilize the high dispersion and resolving power of the Ryerson 30-ft. circle grating spectrograph. This spectrograph permits one to obtain sufficiently precise wave-length measurements of the rotational lines in both bands for accurate measurements of the perturbations.

It was decided that the flow method[12] coupled with high energy input to the discharge tube offered the greatest probability of obtaining a CN flame of high intensity.

Experiments[13] have shown that most carbon compounds are satisfactory, but that the total intensity of the CN bands varies with the compounds used. Likewise, the relative intensities of the violet and red bands show wide variations. Since these effects are very likely caused by secondary processes of energy transfer in the reaction zone, they cannot be predicted, and it is necessary to compare the different compounds experimentally in order to discover the one which yields the CN bands with the greatest intensity. Gases investigated by the writer with respect to the red and violet CN bands were benzene, ethyl iodide, ethyl alcohol, ether, chloroform, carbon tetrachloride, acetone, ethyl acetate, benzaldehyde, pyridine, ethylene, aniline, and formaldehyde. The photographs in this preliminary study were made with a Hilger E-3 quartz spectrograph. The carbon compound finally selected was chloroform, which gave the greatest intensity in both the red and the violet bands. (Pyridine and carbon tetrachloride gave CN bands which were but slightly weaker than those obtained with chloroform.)

The electrical energy was furnished by a 25,000-volt transformer whose load was regulated by inductances in the primary. The power input

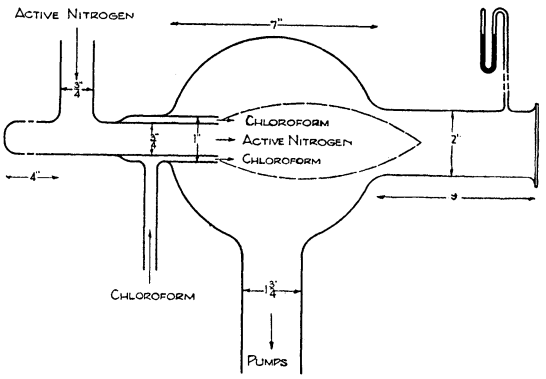

FIG. 1. Afterglow bulb for mixing $CHCl_3$ vapor and active nitrogen issuing separately as indicated from two concentric glass tubes. The resulting flame is photographed through the quartz window fastened by Picein to the end of the nine-inch tube.

varied from 1.5 to 4.5 kva. Power of 2.0 to 2.5 kva was used for the long exposures. Four condensers, in series, of total capacity 0.0025μf, were charged by the transformer and allowed to discharge across a discharge tube in series with a spark gap of about 2-cm separation traversed by a strong air blast. The combined action yielded 3 to 5 sparks during each half-cycle of the alternating current. A heavy grounded wire was connected to the grounded side of the a.c. input, one side of the transformer secondary, one side of the condensers, the discharge tube electrode nearer the pump, the transformer case, the condenser cases, the motor and pump frames, the supporting framework of the apparatus, and the hardware cloth used to protect the power unit.

The discharge tube finally adopted was made of one-inch Pyrex tubing with two sealed-in 150-mil tungsten rods, protected by shorter Pyrex sleeves fastened to the seal. The distance between the electrodes was eight inches. The tube and electrodes were cooled by strong air blasts.

The afterglow tube was made from a two-liter Pyrex bulb (Fig. 1). On one side was sealed a piece of two-inch tubing nine inches long to which a quartz window (two and one-quarter inches in diameter) was fastened by Picein to a flange. Diametrically opposite this window there were two concentric tubes cut off even with each other; the outer tube introduced the chloroform from its container. The active nitrogen and the chloroform vapor mixed as they issued separately

[12] Cf. R. S. Mulliken, Phys. Rev. **26**, 1 (1925).
[13] See references 5–9.

from the concentric tubings and gave a flame which varied from four to eight inches in length, depending on the pressure, relative amounts of the two components, and the power. The flame was directed toward the quartz window, mentioned above, through which the light was photographed. Stray light caused by internal reflections of the light from the discharge tube along the glass tubes was minimized by a set of Rayleigh's horns along the duct of active nitrogen, and light shields were placed externally where necessary.

It was found by experiment that the amount of active nitrogen formed in the discharge tube was so great that a high pumping speed was necessary to utilize it in the afterglow bulb. Two Megavac pumps in parallel were connected to the afterglow bulb by tubing one and three-quarter inches wide, with wide protecting traps cooled by dry ice in acetone, one for each pump.

Tank nitrogen was found to be sufficiently pure for this problem. It was admitted to the discharge tube through a mercury flowmeter and a small stopcock to control the rate of flow, which was about thirty liters per hour. The chloroform vapor was admitted to the mixing tube through a stopcock in a side tube and was used up at the rate of about one cc of liquid per hour. The pressure in the afterglow tube was kept at 4–12 mm mercury. At lower pressures, stray discharges were formed from the discharge tube all the way to the pumps. The flame spectrum then showed admixture of nitrogen bands. The flame was focused on the grating spectrograph by crossed cylindrical lenses in order to give maximum intensity on the plates. A careful check was kept on both the barometric pressure and the temperature of the grating room, so as to forestall any false shifts in the lines. A slit width of 15μ was the minimum used, and 25μ the maximum.

Two 30,000 lines/inch gratings, called No. 2 and No. 3, each with 150,000 lines exposed, mounted on the same circle and using the same slit, were available for this problem. Exposures of the CN bands were made with each grating, as follows for the individual bands: No. 3, λ5598 of the red system, 1st order; λ4216 of the violet system, 1st order; and λ3883 of the violet system, 1st and 2nd orders; No. 2, λ5598, 1st order; λ4216, 1st order; and λ3883, 1st order. The band λ4216 was very weak in 2nd order, and no lines pertaining to λ3593 were obtained with this spectrograph. Eastman Process plates were used for λ3883, 1st and 2nd orders; Eastman 33 plates for λ4216; and Eastman 103-D plates sensitized with ammonia for λ5598.

λ3883, 1st order, could be photographed in one and one-half hours; exposures to 8 or 12 hours brought out the underlying (1,1), (2,2), and (3,3) bands. λ4216, 1st order, required at least eight hours to obtain a strong picture. λ3883, 2nd order, was photographed for a time-period not less than eight hours, and λ5598, 1st order, required at least ten hours.

The standard iron arc was used to calibrate the plates; the iron standards and the band lines were measured with a Geneva comparator. All wave-lengths were reduced to wave numbers in vacuum with the aid of Kayser's "Tabelle der Schwingungzahlen."

DESCRIPTION AND ANALYSIS OF THE DATA

The two plates, one of the 9,4 red band and one of the 0,0 violet band, on which the frequency data reported later are based, were obtained with the No. 3 grating. Both bands were photographed during a single exposure taken with a pressure of about 3–4 mm in the mixing bulb. Other plates, obtained during different exposures, were also measured and the results reported later were checked against these to insure accuracy.

The 0,0 Violet Band

The CN $^2\Sigma(0,0)$ band was measured some years ago by Uhler and Patterson[14] under fairly high dispersion using a carbon arc source, and the wave numbers calculated from their data are given by Herzberg.[15] New measurements made on the second-order plate, with a dispersion of 0.368A/mm, yield essentially the same formula as that given by Herzberg;[15] the equation for the band lines obtained from the present measurement is:

$$\nu = 25{,}797.848 + 3.850m + 0.06796m^2 - 0.000026m^3 - 0.00000022m^4, \quad (1)$$

[14] Uhler and Patterson, Astrophys. J. **42**, 434 (1915).

[15] G. Herzberg. *Molecular Spectra and Molecular Structure, I. Diatomic Molecules* (Prentice-Hall, Inc., New York, 1939), pp. 44–46.

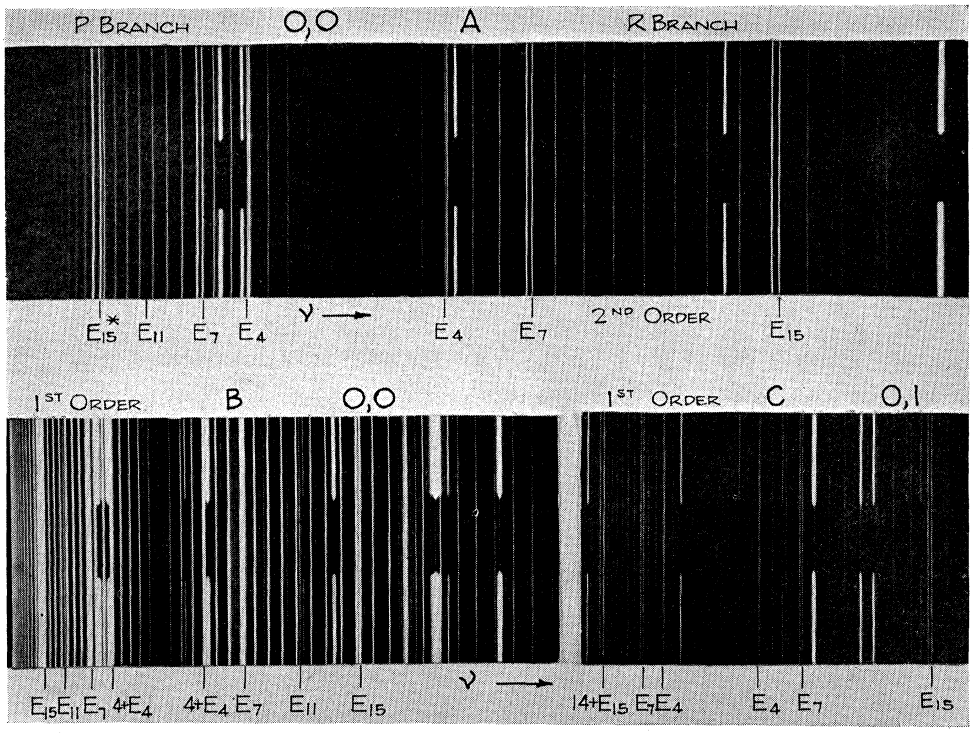

FIG. 2. Bands of the violet CN system. *A*. The 0,0 violet band, second order. The branches are indicated above. Below, four extra lines in the *R* branch and three in the *P* branch are marked. *B*. The 0,0 violet band, first order, over-exposed. Extra lines are marked as in *A*. E_{11} is strong in each branch. The underlying bands of 1,1 and 2,2 violet appear here. *C*. The 0,1 violet band, first order. E_{11} is not visible in enlargement, but appears as very weak line on plate. E_{15} blends with $K'(14)$ in *P* branch. Enhancements of the perturbed lines and the extra lines are apparent in both *A* and *C*. The plates from which these enlargements were made were photographed during the same exposure, with a pressure of 3–4 mm in the afterglow bulb.
* Upper state numbering is used throughout.

where ν refers to centers of doublets. In addition to the lines represented by this formula, the plate shows clearly the four extra lines expected at $K'=4$, 7, 11, and 15 in the *P* as well as in the *R* branch. The separations of these extra lines from the main lines at $K'=4$, 7, 11, and 15 were $\Delta\nu=-0.352$ cm^{-1}, $+0.938$ cm^{-1}, $+1.177$ cm^{-1}, and $+1.212$ cm^{-1}, respectively. Measurements made on other first- and second-order plates of the (0,0) band are in agreement.

Further proof that the perturbed levels belong to the upper state of the 0,0 transition appears in photographs of the 0,1 (λ4216) transition, which show the four extra lines at the same separations from the proper K' band lines in both branches.

The relative intensities of the perturbed and extra lines are dependent on the pressure in the mixing chamber of the apparatus. At high pressures of nitrogen, 8 mm of Hg or greater, the extra lines are relatively weak, and the perturbed lines are not much stronger than the other lines of the band; the extra line at $K'=11$ is too faint to be seen with certainty. If the pressure is lower, 3–4 mm, the extra lines and the perturbed lines are both intensified (see Fig. 2), in both bands λ4216 and λ3883. The extra line at $K'=11$ is now unmistakably present, although still much weaker than the other three. It is quite strong on over-exposed first-order plates of the 0,0 band, as can be seen in Fig. 2 (4–8 hr. exposure).

A study of the 0,0 violet band photographed in second order shows that the lines of the band are sharp and single to $K'=7$. They appear slightly diffuse from $K'=7$ to $K'=15$, and are clearly resolved doublets of unequal intensity above $K'=15$. The doublet separation is very nearly constant in the measurable range (to $K'=22$ in the *P* branch and $K'=20$ in the *R*

branch), the average separation being

$$\Delta\nu = 0.211 \pm 0.012 \text{ cm}^{-1}.$$

The lines with higher K' values in the R branch of the 0,0 violet band (on first-order plates) show anomalous intensities and doublings for values of K' from 22 to 29. All the doublets from $R(16)$ through $R(21)$ are strong and well-resolved; $R(22)$ is barely resolved; $R(23)$ is weak and just resolved; $R(24)$ consists of two components of equal intensity; $R(25)$ looks like a broad asymmetrical unresolved line; $R(26)$ is just resolved into two components of equal intensity and is much weaker; $R(27)$ is strong, broad, and unresolved; and $R(28)$ and $R(29)$ consist of well-resolved components of unequal intensity. Lines with higher values of K' are obscured and partly blended with the lines of the underlying 2,2 and 3,3 bands. These effects cannot be checked on the P branch because the head is formed in this region of K'. A comparison with higher K' members of the 0,1 band was not possible because $K'=21$ was the last one that was obtainable with measurable intensity.

To explain these anomalies, a study of perturbations possible in this region was made. The terms of the $a^2\Sigma$, $v=14$ state lie near the $b^2\Sigma, v=0$ terms; a graph in which extrapolated B_v values of the terms of these two systems are plotted against $K(K+1)$ showed that the term-curves cross at about $K=34$. The energy difference at the K values mentioned above is still approximately 200 cm^{-1}, a value too large to explain the observed anomalies on the basis of the usual type of rotational perturbation. There may be secondary processes which cause this effect; to investigate it may require that one mix different substances with the active nitrogen and operate the mixing tube at different pressures. It is also possible that blends with the underlying 1,1, 2,2, or 3,3 bands may account for these anomalies. Photographs of the 0,0 violet bands with a stronger light source and with greater dispersion would be necessary to check this possibility.

The 9,4 Red Band

The rotational structures of several red bands of cyanogen [(4,1), (5,2), (6,1), (6,2), (7,2), (7,3), and (8,3)] were measured in 1932.[16] The method of analysis used in that report was adopted in the study of the $^2\Pi-{}^2\Sigma$ 9,4 band, whose upper level is the cause of the perturbations mentioned earlier in the $^2\Sigma-{}^2\Sigma$ 0,0 band. The $^2\Pi$ state is an inverted one intermediate between case a and case b. The following branches appear in emission:

$^2\Pi_{3/2}$ to $^2\Sigma$: $R_1(J)$; $Q_1(J)+{}^QR_{12}(J)$; $P_1(J)+{}^PQ_{12}(J)$; and ${}^OP_{12}(J)$;
$^2\Pi_{1/2}$ to $^2\Sigma$: ${}^SR_{21}(J)$; $R_2(J)+{}^RQ_{21}(J)$; $Q_2(J)+{}^QP_{21}(J)$; and $P_2(J)$.

In this band the ${}^SR_{21}$ and the ${}^OP_{12}$ branches are weak but measurable, but the satellite branches are not resolved from the main branches. Eight branches, therefore, were measured and analyzed for this band.

Table I contains the wave numbers in vacuum of the measured lines of the branches of this band and of the differences between the measured frequencies and the calculated frequencies ($\nu_{\text{obs}} - \nu_{\text{calc}}$), based on the constants given below.

The wave numbers of the lines were calculated as the differences between the terms of the $^2\Pi$ and the $^2\Sigma$ levels, each being determined separately. The following equations, the constants of which were obtained as described below, yielded the term values used.

$$\begin{aligned}
^2\Pi_{3/2}:\ T'_{1d}(J) &= 26{,}872.810 \\
&\quad +1.5312\{(J+\tfrac{1}{2})^2-1 \\
&\quad -\tfrac{1}{2}[4(J+\tfrac{1}{2})^2-1{,}267.627]^{\frac{1}{2}}\} \\
&\quad -7.408\times10^{-6}J^4, \\
^2\Pi_{1/2}:\ T'_{2d}(J) &= 26{,}872.810 \\
&\quad +1.5312\{(J+\tfrac{1}{2})^2-1 \\
&\quad +\tfrac{1}{2}[4(J+\tfrac{1}{2})^2-1{,}267.627]^{\frac{1}{2}}\} \\
&\quad -7.408\times10^{-6}(J+1)^4, \\
^2\Sigma:\quad T''_1(J) &= 9{,}042.415 \\
&\quad +1.8202J^2+0.003(J-\tfrac{1}{2}) \\
&\quad -6.44\times10^{-6}J^4, \\
^2\Sigma:\quad T''_2(J) &= 9{,}042.415+1.8202(J+1)^2 \\
&\quad -0.003(J+\tfrac{1}{2}) \\
&\quad -6.44\times10^{-6}(J+1)^4.
\end{aligned} \tag{2}$$

The rotational constants for the $b^2\Sigma$, $v=0$ and $a^2\Sigma$, $v=4$ states were determined by plotting

[16] Jenkins, Roots, and Mulliken, Phys. Rev. **39**, 16 (1932).

TABLE I. Wave numbers* of the lines of the 9,4 band.

J'	R_1	ν(obs.) $-\nu$(calc.)	P_1	ν(obs.) $-\nu$(calc.)	Q_1	ν(obs.) $-\nu$(calc.)	${}^0P_{12}$	ν(obs.) $-\nu$(calc.)
$1\frac{1}{2}$	17,807.157	+0.053	17,796.166	−0.011	17,803.512	+0.051	17,785.130	(−0.142)
$2\frac{1}{2}$	810.956	+0.052	792.755	+0.058	803.666	+0.045	778.350	(+0.191)
$3\frac{1}{2}$	814.104	+0.060	788.607	+0.049	*p* 803.128	+0.004	*p* 770.759	(+0.370)
$4\frac{1}{2}$	816.566	+0.045	783.820	+0.064	802.017	+0.053	762.267	(+0.309)
$5\frac{1}{2}$	818.413	+0.066	778.350	+0.045	800.201	+0.046		
$6\frac{1}{2}$	819.585	+0.066	772.281	+0.079	797.727	+0.032	743.077	−0.077
$7\frac{1}{2}$	*p* 820.204	+0.161	*p* 765.662	+0.208	794.615	+0.026	733.035	(+0.253)
$8\frac{1}{2}$	819.942	+0.021	758.071	+0.011	790.875	+0.033	721.754	−0.018
$9\frac{1}{2}$	819.128	−0.031	750.048	+0.019	786.459	+0.005	710.264	+0.048
$10\frac{1}{2}$	817.756	−0.003	741.372	+0.006	781.436	−0.002		
$11\frac{1}{2}$	815.723	−0.002	732.079	+0.011	775.766	−0.022	${}^0P_{12}$ lines very weak.	
$12\frac{1}{2}$	813.068	+0.007	722.141	−0.005	769.464	−0.051		
$13\frac{1}{2}$	809.763	−0.006	711.582	−0.056	762.570	−0.049		
$14\frac{1}{2}$	805.838	−0.018	700.355	−0.055	755.051	−0.055		
$15\frac{1}{2}$	801.277	−0.041			746.897	−0.076		
$16\frac{1}{2}$	796.166	−0.001			738.144	−0.089		
$17\frac{1}{2}$	790.130	−0.015			728.777	−0.101		
$18\frac{1}{2}$	784.002	−0.006			718.734	−0.128		
$19\frac{1}{2}$	777.019	+0.007			708.190	−0.159		

J'	R_2	ν(obs.) $-\nu$(calc.)	P_2	ν(obs.) $-\nu$(calc.)	Q_2	ν(obs.) $-\nu$(calc.)	${}^SR_{21}$	ν(obs.) $-\nu$(calc.)
$\frac{1}{2}$			( )	( )	17,853.528	−0.070		
$1\frac{1}{2}$	17,858.284	−0.043	(17,840.326)	(+0.194)	850.971	−0.049	17,861.801	(−0.224)
$2\frac{1}{2}$	858.937	+0.021	833.384	−0.058	847.928	−0.029	866.153	+0.007
$3\frac{1}{2}$	858.937	−0.034	826.270	+0.014	844.343	−0.056	869.871	+0.010
$4\frac{1}{2}$	858.580	+0.008	818.555	−0.023	840.326	−0.020	873.113	+0.032
$5\frac{1}{2}$	857.677	−0.022	810.365	−0.029	835.753	−0.019	875.801	−0.004
$6\frac{1}{2}$	856.270	−0.016	801.713	+0.004	830.705	−0.025	877.943	−0.062
$7\frac{1}{2}$	854.357	−0.004	792.518	+0.006	825.173	+0.010	879.688	−0.016
$8\frac{1}{2}$	851.937	+0.013	782.804	−0.002	819.128	+0.043	880.903	+0.011
$9\frac{1}{2}$	848.982	+0.017	772.590	+0.006	812.510	+0.018	881.572	+0.010
$10\frac{1}{2}$	*p* 845.531	+0.049	*p* 761.862	+0.024	805.402	+0.024	881.805	+0.105
$11\frac{1}{2}$	841.522	+0.048	750.603	+0.032	797.727	−0.014	881.370	+0.045
$12\frac{1}{2}$	836.973	+0.042	738.829	+0.055	789.608	+0.031	880.504	+0.090
$13\frac{1}{2}$	831.932	+0.079	726.498	+0.056	780.928	+0.047	879.023	+0.057
$14\frac{1}{2}$	826.302	−0.039	713.648	−0.029	771.722	−0.023	877.099	+0.022
$15\frac{1}{2}$	820.204	+0.140	700.355	+0.183	*p* 762.267	+0.411	*p*	
$16\frac{1}{2}$	813.490	+0.148	686.300	+0.079	751.592	+0.031	871.647	+0.281
$17\frac{1}{2}$					740.764	+0.069		
$18\frac{1}{2}$					729.374	+0.100		
$19\frac{1}{2}$								

* Estimated error = ±0.015 cm^{-1}.
p denotes perturbed lines.

$\Delta_2F/(4J+2)$ against $(J+\frac{1}{2})^2$.[17] The slope of the resulting straight line yields $2D_v$, and the intersection with the ordinate axis gives B_v.

This method, however, does not apply equally well for the $^2\Pi$ state because the rotational formula is more complicated on account of the transition of the coupling from case *a* to case *b* within the range of observed low rotational terms. Therefore, the procedure described below was adopted. Formulas for $\Delta_2F'_1(J)$ and $\Delta_2F'_2(J)$ were obtained from Eq. (2) and then added; the formula which results for the $^2\Pi$ state is

$$[\Delta_2F'_{1d}(J)+\Delta_2F'_{2d}(J)]/(4J+2) = 2B'_v+4D'_v(J^2+J+2).$$

The quantity on the left of this equation when plotted against (J^2+J+2) yields a straight line whose intersection with the ordinate axis is $2B'_v$ and whose slope is $4D'_v$. $B'_9=1.5312\pm0.0008$ cm^{-1} and $D'_9=7.408\pm0.002\times10^{-6}$ cm^{-1} were the values thus obtained for the rotational constants of the $^2\Pi$, $v=9$ state.

[17] Reference 15, p. 191–204.

The experimental value of A, the separation of the electronic $^2\Pi$ sub-levels, was determined from the relation[18]

$$A=T'_2(\tfrac{1}{2})-T'_1(1\tfrac{1}{2})+B'_v-3B'^2_v/A. \quad (3)$$

The numerical value obtained is $A_9=-51.41$ cm^{-1}, in line with those given earlier for the red cyanogen bands, as follows:[19]

$$A_4=-52.14 \text{ cm}^{-1}, \quad A_5=-52.33 \text{ cm}^{-1},$$
$$A_6=-52.52 \text{ cm}^{-1}, \quad A_7=-50.89 \text{ cm}^{-1},$$

and

$$A_8=-51.65 \text{ cm}^{-1}.$$

Λ-Doubling

The Λ-doublings in the $^2\Pi$ states are defined as differences in term value of sub-levels with equal J values, as follows:

$$\Delta\nu_{dc}=T_d(J)-T_c(J),$$

the subscripts c and d having the significance assigned to them by Mulliken.[20] The magnitudes of the doubling can be evaluated from the differences of observed band lines, as follows:

$$^2\Pi_{1/2}: [R_2(J)-Q_2(J)]-[Q_2(J+1)-P_2(J+1)]\sim 2\Delta\nu_{2dc}(J+\tfrac{1}{2}), \quad (4)$$
$$^2\Pi_{3/2}: [R_1(J)-Q_1(J)]-[Q_1(J+1)-P_1(J+1)]\sim 2\Delta\nu_{1dc}(J+\tfrac{1}{2}).$$

The theoretical expressions for the Λ-doubling for cases intermediate between case a and case b are as follows:

$$\Delta\nu_{2dc}=[(\tfrac{1}{2}p_0+q_0)(1+2X^{-1}-YX^{-1}) +2q_0X^{-1}(J-\tfrac{1}{2})(J+1\tfrac{1}{2})](J+\tfrac{1}{2}), \quad (5)$$
$$\Delta\nu_{1dc}=[(\tfrac{1}{2}p_0+q_0)(-1+2X^{-1}-YX^{-1}) +2q_0X^{-1}(J-\tfrac{1}{2})(J+1\tfrac{1}{2})](J+\tfrac{1}{2}),$$

where $Y=A/B_v$, $X=|[Y(Y-4)+(J+\tfrac{1}{2})^2]^{\frac{1}{2}}|$, and p_0 and q_0 are coefficients independent of J which are characteristic of the particular electronic and vibrational state. The constants obtained from the data for $v'=9$ were: $p_0=+0.01597$ and $q_0=-0.00080$. Figure 3 shows the comparison between the observed and calculated values of $\Delta\nu_{idc}$ for the initial state $v'=9$. A study of the graph shows that the observed values of $\Delta\nu_{idc}$'s exhibit large deviations around the J numbers where perturbations occur. The $\Delta\nu_{idc}$'s obtained from this graph were used in evaluating T'_{1c} and T'_{2c} by adding $\Delta\nu$'s to T'_{1d} and T'_{2d} as given by Eq. (2).

Perturbations

It was stated earlier that four extra lines appear in the P and R branches of the 0,0 band of the violet system, and that a calculation performed by Beutler and Fred,[3] using constants for the $^2\Pi$, $v=9$ state obtained by extrapolation, had indicated that the perturbation was caused by the levels of the latter. The just-obtained analysis of the $^2\Pi$, $v=9$ state confirms this conclusion, as will be shown quantitatively.

The terms of the $b^2\Sigma$, $v=0$ state were calculated and compared with those of the $^2\Pi$ state. The graph in Fig. 4, with $J(J+1)$ values as abscissae and T values as ordinates, shows the $^2\Sigma$ state broken into its two components, with J equal to $(K+\tfrac{1}{2})$ and $(K-\tfrac{1}{2})$, and the states $^2\Pi_{3/2}$ and $^2\Pi_{1/2}$. In this diagram each sequence of rotational levels forms very approximately a straight line, and there are four points of intersection, close to $J'=3\tfrac{1}{2}$, $7\tfrac{1}{2}$, $10\tfrac{1}{2}$, and $15\tfrac{1}{2}$.

Each of these J values is the crossing point of two sub-levels, and the correlation is as follows (see Table II).

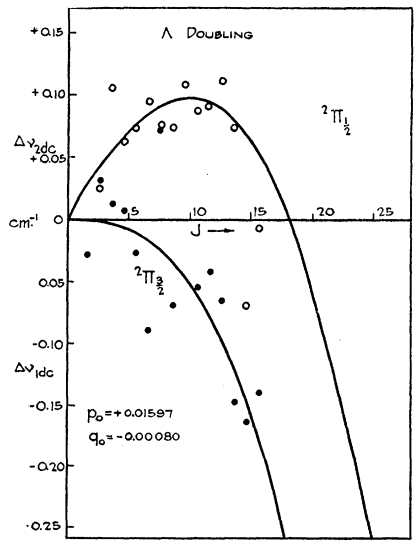

FIG. 3. Λ-doubling in the $^2\Pi$, $v=9$ state. The heavy lines are the theoretical curves obtained with the coefficients given. The circles represent the values of $\Delta\nu_{2dc}(^2\Pi_{1/2})$ obtained from the main branches; the dots the values of $\Delta\nu_{1dc}(^2\Pi_{3/2})$ obtained similarly.

[18] R. S. Mulliken, Phys. Rev. **33**, 747 (1929).
[19] Reference 16, p. 32.
[20] R. S. Mulliken, Rev. Mod. Phys. **3**, 94 (1931).

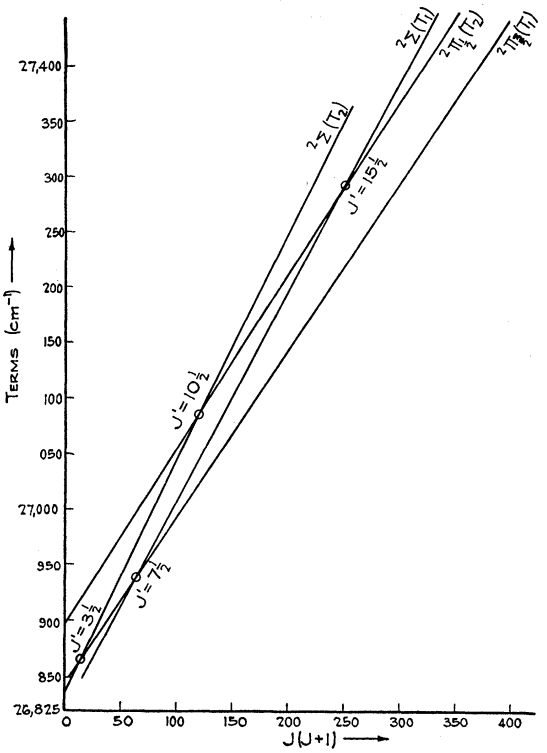

FIG. 4. Curves showing crossing points of terms of $b^2\Sigma$, $v=0$ and of $^2\Pi_{3/2}$ and $^2\Pi_{1/2}$. The $^2\Sigma$ state is broken into its two components, $(K+\frac{1}{2})$ and $(K-\frac{1}{2})$. The four points of intersection are close to $J'=3\frac{1}{2}$, $7\frac{1}{2}$, $10\frac{1}{2}$, and $15\frac{1}{2}$.

The respective parities of the perturbing levels are designated in the sixth column of Table II. In $^2\Sigma$, only one of the two neighboring sub-levels associated with a given K and having equal parity, but which have $J=K+\frac{1}{2}$ or $K-\frac{1}{2}$, will be perturbed. In $^2\Pi_{1/2}$ or $^2\Pi_{3/2}$, however, only one of the two component levels, differing in parity, of the Λ-doublet belonging to a given J will be perturbed. The band lines involving these $^2\Pi$ sub-levels are found in various branches of the 9,4 red band, as follows (cf. Fig. 4):

$^2\Pi_{3/2}$, $J'=3\frac{1}{2}$ (parity +): $Q_1[3\frac{1}{2}]$, $^OP_{12}[3\frac{1}{2}]$,
$J'=7\frac{1}{2}$ (parity −): $R_1[7\frac{1}{2}]$, $P_1[7\frac{1}{2}]$,
$^2\Pi_{1/2}$, $J'=10\frac{1}{2}$ (parity −): $R_2[10\frac{1}{2}]$, $P_2[10\frac{1}{2}]$,
$J'=15\frac{1}{2}$ (parity −): $Q_2[15\frac{1}{2}]$, $^SR_{21}[15\frac{1}{2}]$.

Note: [ ] denote upper state J.

The observations in the satellite branches $^OP_{12}$ and $^SR_{21}$ suffer from lack of intensity. For the other branches, given above, Table I shows that the $\nu_{obs}-\nu_{calc}$ is greater for these lines than for their neighbors, indicating the existence of perturbations.

The differences of the calculated unperturbed terms between $^2\Pi_{3/2}$ and $^2\Sigma$, and $^2\Pi_{1/2}$ and $^2\Sigma$, respectively, are given in column seven of Table II.

The smaller the energy difference between the unperturbed levels (column seven, Table II), the larger, other things being equal, the perturbation that is to be expected and the larger in wave mechanics the mixing of the unperturbed eigenfunctions. The observable results expected from mixing are shifts of the levels and the sharing of transition probabilities between the two states which mix. For a 50 percent mixing, the two levels will exhibit equal probabilities in all their transitions. Extra band lines may appear, whose relative intensities should be a measure of the amount of perturbation.

These viewpoints may first be applied qualitatively to the band lines and extra lines in the violet bands. The value ΔT for $J'=10\frac{1}{2}$ is the largest in Table II, and the connected perturbation is the weakest; this agrees with the experiments (see above). The perturbations at $J'=3\frac{1}{2}$ and $7\frac{1}{2}$ are moderately strong. The perturbation at $J'=15\frac{1}{2}$ is the strongest, as expected, because here the two perturbing levels are moderately close together at a large value of J. In all cases, the extra lines are weaker than the regular lines, indicating that the perturbation never reaches the value of 50 percent mixing in the eigenfunctions.

TABLE II. Unperturbed terms of $b^2\Sigma$, $v=0$, and $^2\Pi$, $v=9$ (cm^{-1}), based on Eq. (1) for $^2\Sigma$ and Eq. (2) for $^2\Pi$.

J	$^2\Sigma(T_2)$	$^2\Sigma(T_1)$	$^2\Pi_{1/2}(T_2)$	$^2\Pi_{3/2}(T_1)$	Parity	$T(^2\Pi)-T^2(\Sigma)$
$3\frac{1}{2}$	26,868.167			26,867.844	+	−0.323
$7\frac{1}{2}$		26,938.673		26,939.368	−	+0.695
$10\frac{1}{2}$	27,087.461		27,088.466		−	+1.005
$15\frac{1}{2}$		27,298.763	27,299.315		−	+0.552

For the $^2\Pi$, $v=9$ levels it is expected that there will be corresponding shifts and extra lines. The shifts are apparent for the lines $Q_1[3\frac{1}{2}]$, $R_1[7\frac{1}{2}]$, $P_1[7\frac{1}{2}]$, $R_2[10\frac{1}{2}]$, $P_2[10\frac{1}{2}]$, and $Q_2[15\frac{1}{2}]$. They confirm completely the perturbations at $K'=4$, 7, 11, and 15 in the violet bands, in that the shifts are in the direction opposite to those in the $b^2\Sigma$, $v=0$ levels, and the term values of the upper levels of the extra lines in $b^2\Sigma$ agree fairly well with those of the $^2\Pi$ system (see Table III).

Exact agreement should exist if all formulas and measurements had been exact. However, the extra lines were not observed in the red band in the intensity expected from analogy with the violet band. The intensity of the red band is rather low, so that variations in intensity would be difficult to determine.

Most of the expected perturbed lines in the 9,4 band were near the heads of the branches to which they belong, or else in a group of other lines which would obscure them. The only line lying isolated is $R_2[10\frac{1}{2}]$, which is the least perturbed; there is no apparent weakening of this line, and no extra line is discernible. If an extra line exists, it would be blended with $Q_2[3\frac{1}{2}]$, as may be shown by calculation. Examination of $Q_2[3\frac{1}{2}]$ under high magnification shows indications of doubling, but considerations below suggest the blended extra line is not really the $R_2[10\frac{1}{2}]$ companion. The corresponding line in the P_2 branch has no measured line in the position where the extra line is expected. $Q_1[3\frac{1}{2}]$ is in the head of the Q_1 branch, and if any extra line were there, it would be completely lost. $R_1[7\frac{1}{2}]$ lies near the head of the R_1 branch, and no conclusion may be drawn, for any extra line would be mixed with $R_1[9\frac{1}{2}]$. $P_1[7\frac{1}{2}]$ is shifted but no extra line is found. $Q_2[15\frac{1}{2}]$, which should be perturbed the most and should give the strongest extra line, is shifted the most, as stated above; however, again no line could be identified definitely as an extra line.

Theory states that a small residual shift occurs in those levels immediately preceding and following the perturbed level when perturbations occur between two rotational levels. To check this quantitatively, a study of the 0,0 violet band was made; this band, as stated earlier, shows the enhancements and extra lines much more strongly than does the 9,4 red band. Figure 5

TABLE III. Term values* of upper levels of extra lines in 0,0 violet and of main lines in 9,4 red (cm^{-1}).

From $^2\Sigma$ data	From $^2\Pi$ data
26,867.838 (T_2)	26,867.804 (T_1)
26,939.522 (T_1)	26,939.553 (T_1)
27,088.629 (T_2)	27,088.491 (T_2)
27,299.781 (T_1)	27,299.740 (T_2)

* These values were obtained by adding $\nu_{obs}-\nu_{calc}$ from Fig. 6 for $^2\Sigma$ or from Table I for $^2\Pi$ data differences to the calculated unperturbed terms of Table II, and for $^2\Sigma$ also adding the observed interval Δ from main to extra line.

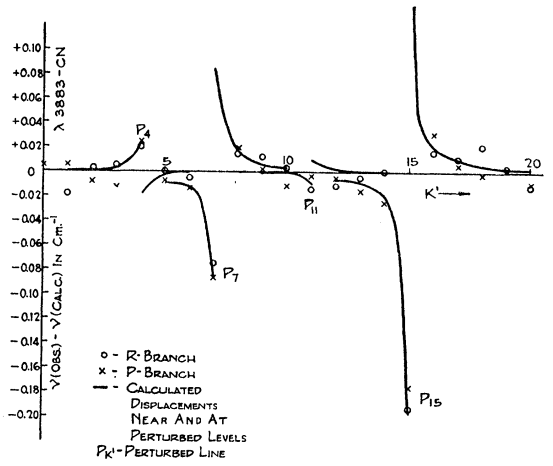

FIG. 5. Graph showing $\nu_{obs}-\nu_{calc}$ for the 0,0 violet band; ν_{calc} is obtained from Eq. (1), adjusted for γ' (see text). Circles represent $\Delta\nu$'s for the R branch, crosses for the P branch. The perturbed lines at $K'=4$, 7, 11, and 15 are indicated by $P_{K'}$. The heavy curves represent the calculated shifts in $\Delta\nu$ near and at each perturbation, given by $\frac{\delta}{2}\pm(S_{RV}^2+\frac{1}{4}\delta^2)^{\frac{1}{2}}$.

shows $\nu_{obs}-\nu_{calc}$ for the 0,0 violet band; the shifts of the perturbed lines are expressed quantitatively here, and comparison of Fig. 5 with Table II and Fig. 4 shows that the shifts following each perturbed line are in the direction expected. The values of $\nu_{obs}-\nu_{calc}$ plotted in Fig. 5 include the adjustment of Eq. (1) for the value of γ' given later. The amount of the adjustment for each line was calculated as a function of K for that line and a correction made for the resultant shift of the center of each unresolved doublet from the uncorrected calculated positions. The values of ν_{obs} for $K'>15$ are for the components of $K'=J'+\frac{1}{2}$.

It is possible to calculate the value of S_{RV}, the perturbing matrix element, from these measured results. In Fig. 6, R and V are mutually perturbing levels of the same J value, δ is the separation of the corresponding unperturbed levels in cm^{-1}, and Δ is the actual separation (measurable as the difference between the main and the extra line in the λ3883 band). The R and V levels are displaced by equal and opposite amounts from their unperturbed positions. The following equation[21]

$$\Delta=(4S_{RV}^2+\delta^2)^{\frac{1}{2}} \qquad (6)$$

[21] L. N. Liebermann, Phys. Rev. **60**, 504 (1941), Eq. (8).

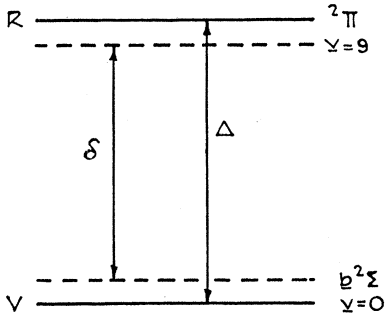

FIG. 6. Schematic diagram of two mutually perturbing levels of the same J value of the red (R) and violet (V) bands of CN. Δ is the actual observed separation of R and V (equal to the separation of a main and corresponding extra line in a violet band) and δ is the corresponding separation of the unperturbed levels in cm^{-1}.

expresses the relation between the known Δ and the unknown S_{RV} and δ.

Since

$$\Delta=\nu(E_V)-\nu(M_V)$$

and

$$\tfrac{1}{2}(\Delta-\delta)=\nu^0(M_V)-\nu(M_V),$$

$(\Delta-\delta)$ and $(\Delta+\delta)$ may be calculated from the observed wave numbers of the perturbed main and extra lines (M and E) of the violet bands, combined with the unperturbed values ν_0 of the main lines taken from a graph or equation for the unperturbed lines. Using the values of Δ given just below Eq. (1) and those of $\frac{1}{2}(\Delta-\delta)$ obtained from Fig. 5, we obtain the following approximate values of S_{RV}^2:

$$S_4^2=0.00758,\quad S_7^2=0.0694,$$
$$S_{11}^2=0.0105,\quad S_{15}^2=0.190.$$

The wave functions of the perturbed levels are

$$\psi_R=(1-\rho^2)^{\frac{1}{2}}\psi_R^0-\rho\psi_V^0,\qquad(7)$$
$$\psi_V=\rho\psi_R^0+(1-\rho^2)^{\frac{1}{2}}\psi_V^0.$$

In the case under consideration, the transitions occur from the upper levels R and V to two lower levels belonging to the $a^2\Sigma$ state, namely, to R'' in $v''=4$ for the red bands and to V'' in $v''=0$ or 1 for the violet CN bands. There will be a "main" line M_R and a weaker "extra" line E_R in the red system bands, and likewise an M_V and an E_V in the violet system bands (see Fig. 7).

Let

$$P_R^0\equiv\left[C\int\psi_R^0P\psi_{R''}^*d\tau\right]^2\equiv a^2,$$
$$P_V^0\equiv\left[C\int\psi_V^0P\psi_{V''}^*d\tau\right]^2\equiv r^2a^2\qquad(8)$$

be the transition probabilities for the unperturbed main lines $R\rightarrow R''$ and $V\rightarrow V''$, respectively. Let it also be supposed that the unperturbed transitions $R\rightarrow V''$ and $V\rightarrow R''$ have negligible intensities. (This seems to be true experimentally.) Then for the actual case

$$M_R:\ P_{RR''}\equiv\left[C\int\psi_RP\psi_{R''}^*d\tau\right]^2=(1-\rho^2)a^2,$$
$$E_R:\ P_{VR''}\equiv\left[C\int\psi_VP\psi_{R''}^*d\tau\right]^2=\rho^2a^2,$$
$$M_V:\ P_{VV''}\equiv\left[C\int\psi_VP\psi_{V''}^*d\tau\right]^2=(1-\rho^2)r^2a^2,\qquad(9)$$
$$E_V:\ P_{RV''}\equiv\left[C\int\psi_RP\psi_{V''}^*d\tau\right]^2=\rho^2r^2a^2.$$

From the theory connecting ρ^2 with S_{RV}^2 and δ^2, one finds [cf. reference 21, Eq. (9)]

$$\rho^2/(1-\rho^2)=(\Delta-\delta)/(\Delta+\delta).\qquad(10)$$

Let the populations of states R and V at any instant be N_R and N_V, respectively. Then, if

$$p\equiv N_R/N_V,\qquad(11)$$

the intensity ratios must be

$$q_V\equiv I(E_V)/I(M_V)=[\rho^2/(1-\rho^2)]N_R/N_V=\left(\frac{\Delta-\delta}{\Delta+\delta}\right)p,$$
$$q_R\equiv I(E_R)/I(M_R)=[\rho^2/(1-\rho^2)]N_V/N_R=\frac{\Delta-\delta}{\Delta+\delta}\left(\frac{1}{p}\right).\qquad(12)$$

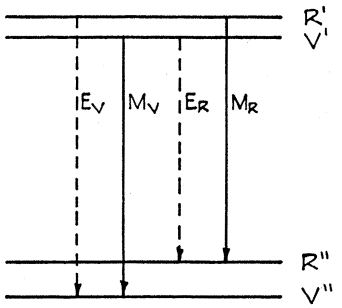

FIG. 7. Schematic diagram showing expected transitions from upper levels R and V to the lower levels R'' in $v''=4$ and V'' in $v''=0$ or 1 for the red and violet CN bands, respectively. The interval $R'-V'$ is actually about three orders of magnitude smaller than $R''-V''$, and its sign in one case is negative. M represents main line and E represents extra line.

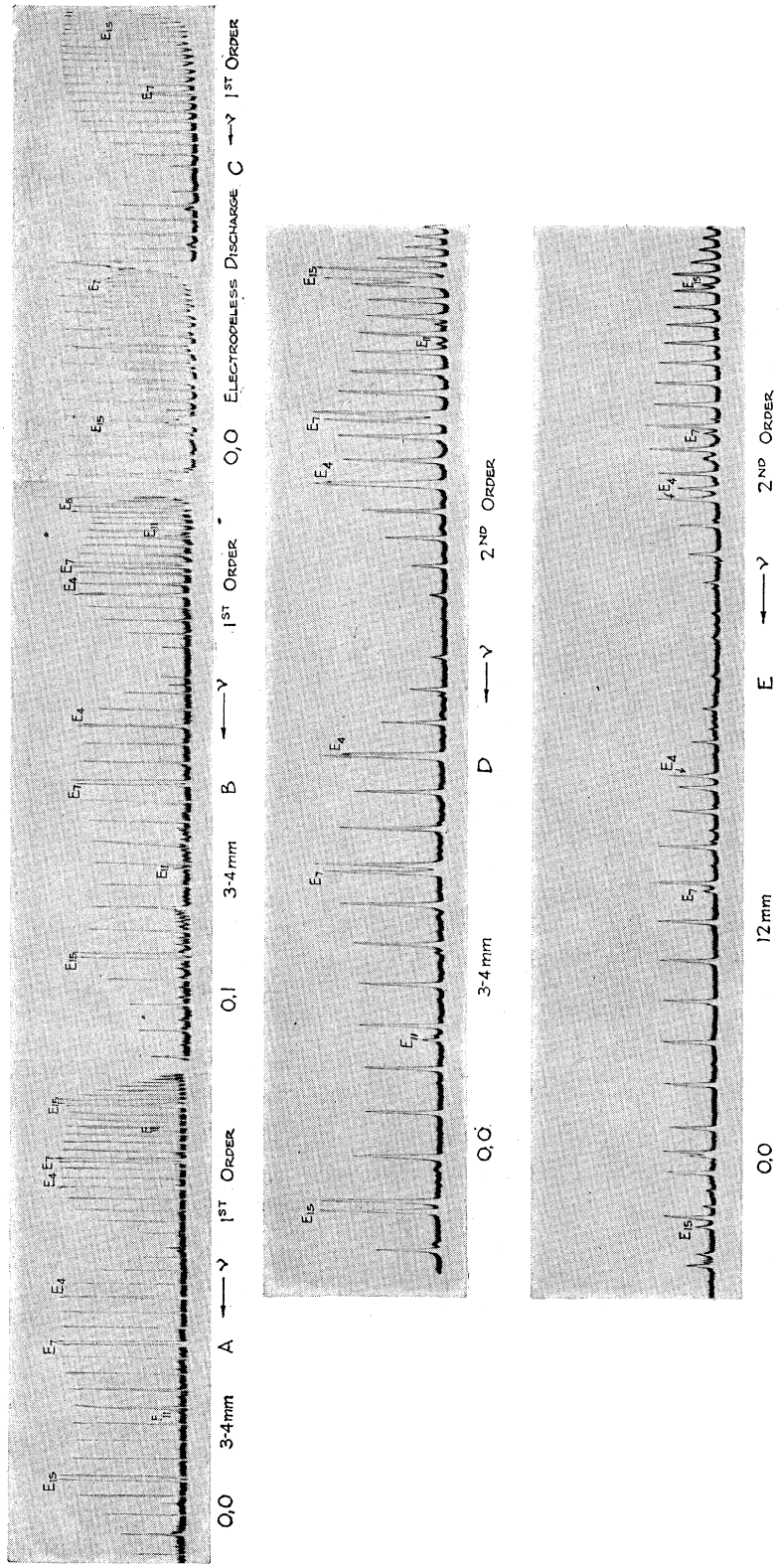

FIG. 8. Microphotometer curves of photographs of violet CN system. R branch on left in all traces, P branch on right. $E_{K'}$ denotes extra lines. The perturbed and extra lines are noticeably enhanced except in traces C and E. Traces A, B, and D are made from plates obtained by mixing $CHCl_3$ with active nitrogen—photographs all made during same exposure. Trace E is from same source operated at higher pressure. Trace C (reference 22) is from plate obtained with stopcock grease as small impurity in electrodeless discharge. Traces C and E show less enhancement of perturbed and extra lines and fewer extra lines.

TABLE IV. Values of $\frac{\Delta-\delta}{\Delta+\delta}$, q_v, $p_{K'}$, ρ^2, and $(1-\rho^2)$ obtained from the 0,0 violet band.

K'	$\Delta-\delta/\Delta+\delta$	q_v	$p_{K'}$	q_R	ρ^2	$1-\rho^2$
4	0.0699	1	14	0.005	0.065	0.935
7	0.0945	1	10	0.0095	0.086	0.914
11	0.0077	1/6	22	0.00035	0.00764	0.99236
15	0.179	1	6	0.0298	0.152	0.848

The microphotometer traces, Fig. 8, give a qualitative measure of q_v. Trace A, λ3883 in first order, and trace B, λ4216 in first order, show that $q_v\sim1$ for the perturbations at $K'=4$, 7, and 15 at a pressure of 3–4 mm and $q_v\ll1$ for the perturbation at $K'=11$. Trace C, taken from a plate made by Dr. S. Mrozowski[22] under radically different discharge conditions (electrodeless discharge in a heated tube containing bismuth vapor at perhaps a few tenths mm pressure, helium at 1- or 2-mm pressure, and a trace of stopcock grease), shows only the extra lines at $K'=7$ and 15, respectively, in λ3883, both with $q_v\ll1$. Trace D is from the same exposure as Trace A (λ3883 at 3–4 mm), but in second order. Trace E shows λ3883 in second order at 12 mm. At this pressure, the extra lines at $K'=7$ and 15, respectively, are the only ones which appear, and the enhancements are very small. Also, $q_v\ll1$ in this case. These relations resemble those on Dr. Mrozowski's plate. Reasons for the variations of q_v, and therefore p, with pressure will be discussed later.

A study of the microphotometer traces shows that $q_v\sim1$ for $K'=4$, 7, and 15, and $q_v\sim1/6$ for $K'=11$ at 3–4 mm. Equation (12) states that

$$q_v=\left(\frac{\Delta-\delta}{\Delta+\delta}\right)p.$$

Substitution of the values of Δ and δ used in the calculation of S^2_{RV} yields experimental values of $p\equiv N_R/N_V$, for the photographs at 3–4-mm pressure (see Table IV). If now these values of p are substituted in the second of Eq. (12), values for q_R can be predicted, and are all found to be 0.03 or less. Thus, on this basis, the experimentally observed absence of extra lines in the red 9,4 band as photographed at 3–4-mm pressure seems to be very satisfactorily explained. At 12-mm pressure, where the photographs of λ3883 indicate that $p=1$ may be approached, one can now predict that the extra lines in the red bands might be visible, but unfortunately no suitable plates of the red bands were obtained under these conditions.

Substitution of the values of ρ^2 and $(1-\rho^2)$ from columns 6 and 7, respectively, in Table IV yields the following transition probabilities as given in Table V. The quantities a^2 and r^2 should be substantially the same for all K values.

Now let $N_V{}^0$ be the population of an unperturbed level ($N_V{}^0$ is, of course, a function of K); then one may define

$$m\equiv N_V/N_V{}^0 \qquad (13)$$

for any perturbed V level. One may determine m approximately by drawing a smooth curve through the least perturbed violet band line intensities to estimate an $N_V{}^0$ for the given perturbed line. Such an estimate obtained with the aid of a microphotometer trace of a band taken at a pressure of 3–4 mm yields: $m_4\sim1.2$, $m_7\sim1.1$, $m_{11}\sim1.0$, and $m_{15}\sim1.25$. In the band obtained by S. Mrozowski (see Fig. 8), it may be observed that $m\sim1.0$ for the two perturbations observed there.

This phenomenon of enhancement of the perturbed main lines and the extra lines in the violet band, and the lack of enhancement or weakening of the perturbed main lines and the absence of the extra lines in the associated red band, requires that a collision process be postulated. The process must be one in which rapid $R\rightarrow V$ transfer occurs at the K values where there are perturbations. Further, it must be such that the perturbed rotational levels of the red band are repopulated by rotational redistribution collisions at about the same rate as they are depopulated by collision transfer to the perturbed

TABLE V. Transition probabilities.

K'	$P_{RR''}$	$P_{VR''}$	$P_{VV''}$	$P_{RV''}$
4	$0.935a^2$	$0.065a^2$	$0.935r^2a^2$	$0.065r^2a^2$
7	$0.914a^2$	$0.086a^2$	$0.914r^2a^2$	$0.086r^2a^2$
11	$0.99236a^2$	$0.00764a^2$	$0.99236r^2a^2$	$0.00764r^2a^2$
15	$0.848a^2$	$0.152a^2$	$0.848r^2a^2$	$0.152r^2a^2$

[22] The author wishes to thank Dr. Mrozowski for his kindness in permitting him to use the plate from which this trace was made.

violet levels and emission in the violet band. This is in agreement with the prediction of Beutler and Fred (cf. reference 3), where the effect of pressure is discussed. The effect would be "smoothed out" at very high or very low pressures. The traces in Fig. 8 obtained from plates (with the exception of S. Mrozowski's) made at medium pressures, indicate that apparently there is such an effect. The "smoothing out" in S. Mrozowski's plate may be caused by a higher temperature in the discharge tube (experimentally true) or by very low partial pressure of the CN present.

It is probable that the colliding molecules which are effective in repopulating the depleted rotational levels are CN molecules. It would be necessary to perform a new set of experiments ranging down to 0.5-mm pressure in order to check completely the effect of pressure; it might even be advisable to use different admixed substances and different temperatures of the mixing tube. The discharge system used here is not suitable for such low pressures because the stray discharge becomes too intense at these pressures.

During the discussion of the 0,0 violet band, it was stated that the doubling in the $^2\Sigma$ state becomes noticeable at $K'=16$. The doublets were observed to have one strong component and one very weak component (see Fig. 9), the strong component being on the higher wave number side. The intensity of this component falls off rapidly, with increasing K, and appears visually to have nearly the same intensity as the weak component at higher $K(K'=20, 21,$ and $22)$. The doublet splitting was measured, and the value of $(\gamma'-\gamma'')$ determined to be $+0.0110$. Birge[23] gives $(\gamma'-\gamma'')=0.0090$ from CN bands obtained with a hot source. Comparison of $(\gamma'-\gamma'')=+0.0110$ with $\gamma''=+0.0104$ obtained by extrapolation from the results of Jenkins, Roots, and Mulliken[24] gives $\gamma'=+0.0214$.

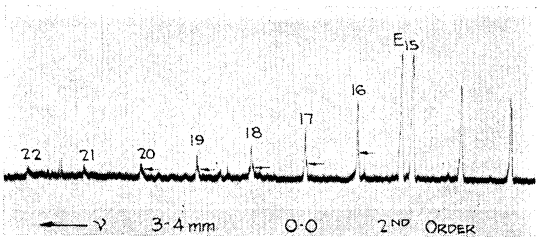

FIG. 9. Microphotometer curve of R branch of 0,0 violet band for larger values of K'. The strong doublet components with $J'=K'+\frac{1}{2}$ and the weak components with $J'=K'-\frac{1}{2}$ appear for $K'\geq 16$; for $K'\geq 20$, both components are weak and of comparable intensity.

The intensification of one series of doublet components may be explained according to the following interesting mechanism. They have $J'=K'+\frac{1}{2}$ like the perturbed line $K'=15$, and are intense because of collision enhancement either directly like the perturbed line, or indirectly as a result of collision enhancement of $J'=15\frac{1}{2}$ followed by collisions which change K' by one or a few units without changing the direction of the spin. The weak doublet components then have $J'=K'-\frac{1}{2}$; their intensity may be near the natural intensity without collision enhancement, or they may also have been enhanced somewhat by collisions, but much less than for $J'=K'+\frac{1}{2}$ because the perturbed lines which have $J'=K'-\frac{1}{2}$ are weak or remote from the $K'=15$ region.

The author wishes to express his appreciation of invaluable advice and criticism of the late Dr. H. G. Beutler and of Professor R. S. Mulliken in the solution of the experimental and theoretical problems involved.

[23] R. T. Birge, Astrophys. J. **55**, 280 (1922).

[24] See reference 16, pp. 29–30.

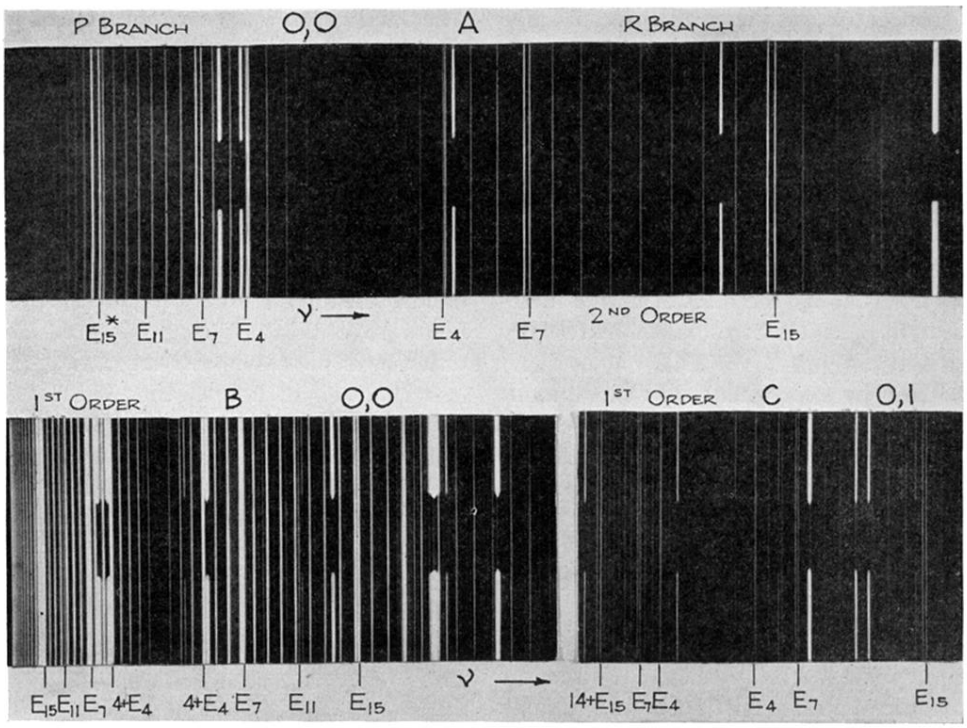

FIG. 2. Bands of the violet CN system. *A*. The 0,0 violet band, second order. The branches are indicated above. Below, four extra lines in the *R* branch and three in the *P* branch are marked. *B*. The 0,0 violet band, first order, over-exposed. Extra lines are marked as in *A*. E_{11} is strong in each branch. The underlying bands of 1,1 and 2,2 violet appear here. *C*. The 0,1 violet band, first order. E_{11} is not visible in enlargement, but appears as very weak line on plate. E_{15} blends with $K'(14)$ in *P* branch. Enhancements of the perturbed lines and the extra lines are apparent in both *A* and *C*. The plates from which these enlargements were made were photographed during the same exposure, with a pressure of 3–4 mm in the afterglow bulb.

* Upper state numbering is used throughout.

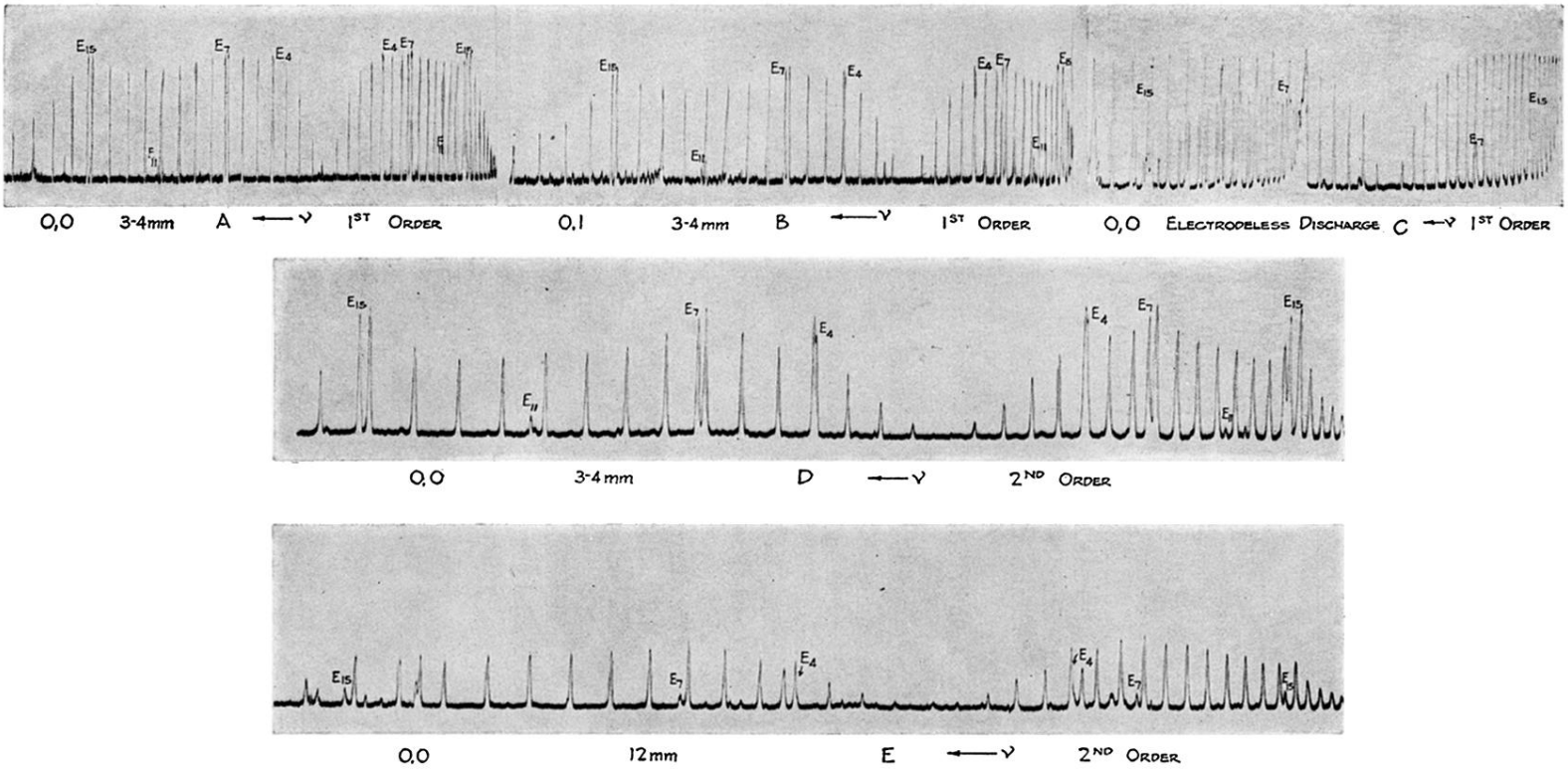

FIG. 8. Microphotometer curves of photographs of violet CN system. *R* branch on left in all traces, *P* branch on right. $E_{K'}$ denotes extra lines. The perturbed and extra lines are noticeably enhanced except in traces *C* and *E*. Traces *A*, *B*, and *D* are made from plates obtained by mixing $CHCl_3$ with active nitrogen—photographs all made during same exposure. Trace *E* is from same source operated at higher pressure. Trace *C* (reference 22) is from plate obtained with stopcock grease as small impurity in electrodeless discharge. Traces *C* and *E* show less enhancement of perturbed and extra lines and fewer extra lines.

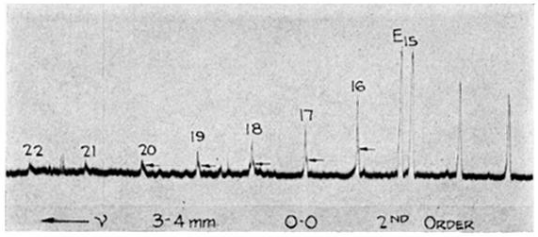

FIG. 9. Microphotometer curve of R branch of 0,0 violet band for larger values of K'. The strong doublet components with $J'=K'+\frac{1}{2}$ and the weak components with $J'=K'-\frac{1}{2}$ appear for $K'\geq 16$; for $K'\geq 20$, both components are weak and of comparable intensity.